Structural elucidation of the binding and inhibitory properties of lanthanide (III) ions at the 3′–5′ exonucleolytic active site of the Klenow fragment

Chad A Brautigam[1]*, Kathryn Aschheim[1] and Thomas A Steitz[1,2]

Background: Biochemical and biophysical experiments have shown that two catalytically essential divalent metal ions (termed 'A' and 'B') bind to the 3′–5′ exonuclease active site of the Klenow fragment (KF) of *Escherichia coli* DNA polymerase I. X-ray crystallographic studies have established the normal positions in the KF 3′–5′ exonuclease (KF exo) active site of the two cations and the single-stranded DNA substrate. Lanthanide (III) luminescence studies have demonstrated, however, that only a single europium (III) ion (Eu^{3+}) binds to the KF exo active site. Furthermore, Eu^{3+} does not support catalysis by KF exo or several other two-metal-ion phosphoryl-transfer enzymes.

Results: A crystal structure of KF complexed with both Eu^{3+} and substrate single-stranded oligodeoxynucleotide shows that a lone Eu^{3+} is bound near to metal-ion site A. Comparison of this structure to a relevant native structure reveals that the bound Eu^{3+} causes a number of changes to the KF exo active site. The scissile phosphate of the substrate is displaced from its normal position by about 1 Å when Eu^{3+} is bound and the presence of Eu^{3+} in the active site precludes the binding of the essential metal ion B.

Conclusions: The substantial, lanthanide-induced differences in metal-ion and substrate binding to KF exo account for the inhibition of this enzyme by Eu^{3+}. These changes also explain the inability of KF exo to bind more than one cation in the presence of lanthanides. The mechanistic similarity between KF exo and other two-metal-ion phosphoryl-transfer enzymes suggests that the principles of lanthanide (III) ion binding and inhibition ascertained from this study will probably apply to most members of this class of enzymes.

Addresses: [1]Department of Molecular Biophysics and Biochemistry and [2]Department of Chemistry, Howard Hughes Medical Institute, Yale University, PO Box 208114, New Haven, CT 06520-8114, USA.

*Present address: Howard Hughes Medical Institute, The University of Texas Southwestern Medical Center at Dallas, 5323 Harry Hines Boulevard, Dallas, TX 75235-9050, USA.

Correspondence: Thomas A Steitz

Key words: europium (III), 3′–5′ exonuclease, lanthanide (III), two-metal-ion mechanism, X-ray crystallography

Received: 21 July 1999
Revisions requested: 20 August 1999
Revisions received: 22 September 1999
Accepted: 23 September 1999

Published: 16 November 1999

Chemistry & Biology December 1999, 6:901–908

1074-5521/99/$ – see front matter

Introduction

The 3′–5′ exonuclease of the large fragment (Klenow fragment, KF) of DNA polymerase I from *Escherichia coli* typifies a class of enzymes that uses two divalent metal cations as cofactors to catalyze the hydrolysis of a phosphodiester bond. Numerous biochemical and X-ray crystallographic experiments [1–5] have established that substrate single-stranded DNA (ssDNA) binds to the active site of the enzyme along with two divalent metal ions (termed 'A' and 'B'), and that both metal ions are necessary for catalysis. These cations are proposed to bind and orient an incoming nucleophile and to stabilize both the pentacoordinated transition state and the negative charge on the leaving oxyanion [3,4] (Figure 1). A number of other phosphoryl-transfer enzymes have been proposed to utilize a similar mechanism [6], including DNA polymerases [7–10], adenylyl cyclase [11,12], alkaline phosphatase [13], the RNaseH domain of HIV-1 reverse transcriptase [14], inositol monophosphatase [15–17] and ribozymes [18]. The active site of the 3′–5′ exonuclease of KF (KF exo) permits Mg^{2+}, Mn^{2+}, Zn^{2+} and Co^{2+} to bind to the active site and to serve in the KF exo-catalyzed hydrolysis of DNA [1–5,19–22]. Despite this flexibility, the lanthanide (III) cation europium (Eu^{3+}) acts as a competitive inhibitor with respect to Mg^{2+} in the KF exo reaction [23]. Several other two-metal-ion phosphoryl-transfer enzymes, such as DNA polymerases, are similarly inhibited by Eu^{3+} [23]. Thus, although solution studies show Eu^{3+} can support phosphoryl transfer [24], it must interact with the active sites of these enzymes in a manner that is incompatible with catalysis. Lanthanide (III) (Ln^{3+}) ions have long been used to explore the structure, function and metal-binding properties of proteins [25–28]. The convenient and well-characterized luminescence signal of Eu^{3+} makes it particularly attractive for detecting metal-ion binding to proteins [25,26]. In order to establish whether such cations might be used as probes for metal-ion binding to two-metal-ion phosphoryl-transfer enzymes, Ln^{3+} luminescence studies have been carried out [23]. Although other spectroscopic analyses using smaller, divalent cations have shown that two metal ions bind to the KF exo active site [20,21], lanthanide (III) luminescence studies indicate that only a single Ln^{3+} binds [23]. The binding of a lone Ln^{3+} might explain the inability of KF exo to employ these cations as

Figure 1

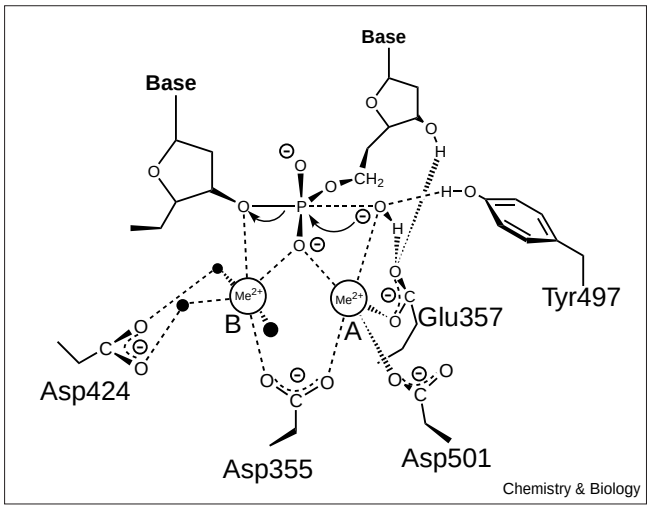

The two-metal-ion mechanism of KF 3′–5′ exonuclease. The nucleophile (shown as OH^- here) is activated by metal ion A and is oriented for attack by this cation and protein sidechains. It attacks the scissile phosphate, generating a pentacoordinated transition state. This state is stabilized by both metal ions. Finally, electrons leave the phosphate and become resident on the leaving oxygen atom. The negative charge on this atom is stabilized by metal ion B. The closed circles represent water molecules in contact with metal ion B. Adapted from [5].

cofactors [23] because structure–function studies of this enzyme have demonstrated that two cations are necessary for catalysis [1,2]. However, the spectroscopic experiments that indicate that only a single Ln^{3+} is binding were performed in the absence of substrates, which have a profound effect on metal-ion binding [1,4,5,29]. Therefore, the exact mechanism by which lanthanides inhibit the exonucleolytic reaction is not fully established.

To provide a structural basis for understanding the binding and inhibitory behavior of Ln^{3+} ions with respect to KF exo, we have solved three X-ray crystal structures of this enzyme in the presence of a lanthanide (III) cation, Eu^{3+}. The first, a 2.2 Å resolution structure of Eu^{3+} bound to the KF exo active site in conjunction with substrate ssDNA, shows a single lanthanide cation bound near to the previously characterized metal-ion site A. Comparison of this structure to a previously determined structure of KF exo containing divalent cations and substrate [5] indicates that significant rearrangements to the active site are induced by Eu^{3+} binding. The other two structures, those of the KF–Eu^{3+} and KF–Eu^{3+}–dTMP (dTMP, deoxythymidine monophosphate) complexes, reveal that a lone Eu^{3+} occupies this active site whether it is present alone or together with dTMP, a product of the exonuclease reaction. These results demonstrate that Eu^{3+} inhibits the enzyme activity of KF exo (and probably other two-metal-ion enzymes)

Table 1

Summary of data collection and refinement.

Parameter	Eu^{3+} alone	Eu^{3+}–product	Eu^{3+}–substrate
Pdb accession number	N/A	N/A	1QSL
Resolution range (Å)	7–3.8	7–3.5	20–2.2
wavelength (Å)	1.54	1.54	0.909
Number of reflections	46678	54346	343566
Number of unique reflections (F > 2 σ)	5636	7257	40431
Completeness (%)	91.8	76.0	99.6
Average I/s	6.0	6.0	16.4
R_{sym}*	0.146	0.143	0.074
Average I/σ (highest res. shell)	1.9	2.2	3.7
R_{sym} (highest res. shell)	0.452	0.299	0.345
Number of protein atoms	4754	4754	4754
Number of water molecules	0	0	191
Final *R* factor	0.267†	0.287	0.214
Final R_{free} factor	0.264	0.296	0.254
Rms deviations			
Bond lengths (Å)	N/A	N/A	0.009
Bond angles (°)	N/A	N/A	1.6
Dihedrals (°)	N/A	N/A	23.4
Impropers (°)	N/A	N/A	1.3

$$*R_{sym} = \frac{\sum_{hkl}\left|I-\hat{I}\right|_{hkl}}{\sum_{hkl} I_{hkl}}$$

where Î represents the mean intensity value for symmetry- (or Friedel-) equivalent reflections, and hkl denotes the irreducible set of reflections within the reciprocal-space asymmetric unit. †Only rigid-body refinement was performed on these structures.

Figure 2

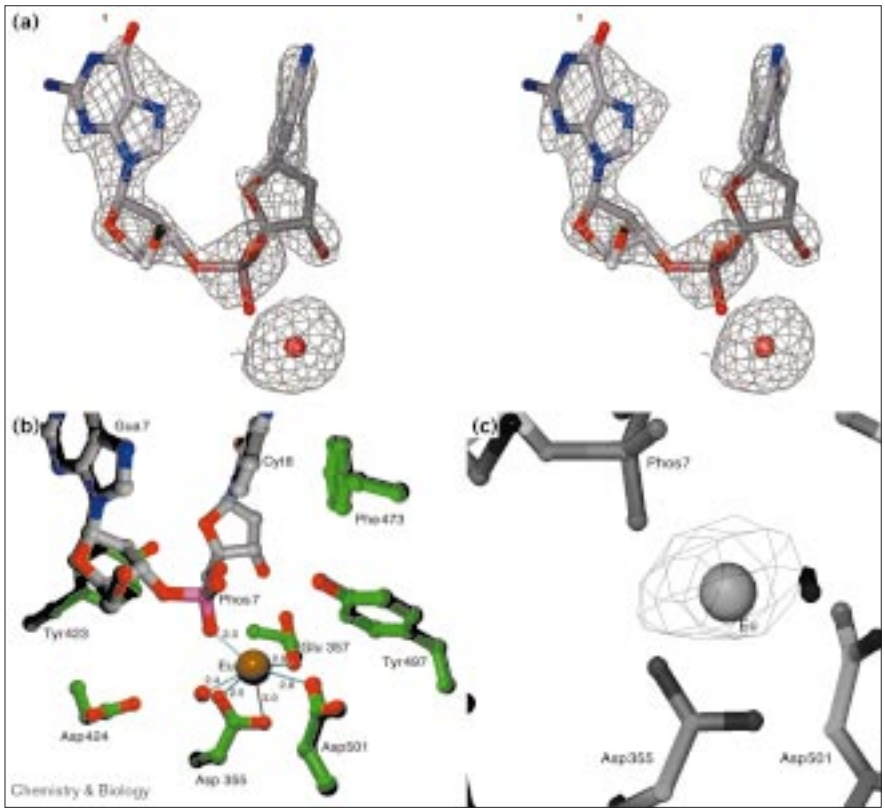

The binding of Eu^{3+} and substrate to KF exo. (a) Stereo diagram of the electron density for the substrate and Eu^{3+}. Shown is a simulated-annealing F_o–F_c omit map [40] in which the 3′-terminal dinucleotide and Eu^{3+} had been omitted from the calculation. The density, contoured at 2.0 σ, is superimposed on the final refined positions of the omitted atoms. Carbon atoms are shown in silver, nitrogens are blue, phosphorus is mauve, and oxygens are red. The Eu^{3+} is shown as an orange sphere. This figure and all others featuring electron density were made using the program O [38]. (b) The configuration of the KF exo active site in the presence of Eu^{3+} and substrate. The color scheme for the atoms is the same as in Figure 2a except that protein carbons are green and the Eu^{3+} is bronze. All distances in this and all other figures are given in angströms. This figure was made in VMD [41] and rendered using POV-Ray. (c) Anomalous difference map for KF exo bound to Eu^{3+} and substrate. This 18 σ peak is observed when data from 10–4.0 Å are used to calculate an anomalous difference map. The map, contoured at 5 σ, is superimposed on the refined Eu^{3+}–substrate coordinates.

because binding of this cation both mispositions the substrate and prohibits the binding of the catalytically essential metal ion B. They also show that the primary reason that only a single metal ion binds to this active site in the presence of Eu^{3+} is that a carboxylate that normally ligates both metal ions A and B interacts exclusively with Eu^{3+}. Finally, this report indicates that although Ln^{3+} ions might serve as probes for metal-ion binding to some two-metal-ion phosphoryl-transfer enzymes, their size and charge cause them to bind differently than the smaller, less charged native divalent cations do.

Results

Eu^{3+}–substrate complex and comparison to the native complex

A crystal structure at 2.2 Å resolution of KF complexed with Eu^{3+} and substrate ssDNA shows that only a single Eu^{3+} can bind concomitantly with ssDNA at the KF exo active site under our crystallographic conditions (Figure 2). This structure (hereafter referred to as the 'Eu^{3+}–substrate complex') has been refined to an R factor of 21.4% and an R_{free} of 25.4% (Table 1). A previous kinetic rate analysis has established that KF exo is essentially inactive in the presence of Eu^{3+} [23]. This allowed us to soak both Eu^{3+} and ssDNA into KF crystals at pH 7.5 for one hour without the enzyme hydrolyzing the substrate. The electron density associated with the substrate and Eu^{3+} is shown in Figure 2a. As in previous experiments [5], only the three most 3′ nucleotides of the DNA are visible in electron-density maps. These nucleotides bind to KF at its ssDNA binding site [3,4] (Figure 2b). The lone Eu^{3+} binds close to the previously characterized metal-ion site A. We have confirmed the identity of the cation using an anomalous difference electron-density map (Figure 2c). Given that Eu^{3+} is the only strong anomalous scatterer present in the crystal, this map should betray the positions of all ordered Eu^{3+} ions. The only peak in this map is close to metal-ion site A. On the basis of the sum of their ionic radii, the expected distance between Eu^{3+} and a liganding oxygen atom is 2.4 Å (1.2 + 1.2 Å). Using this criterion, the ion is well liganded by one of the carboxylate oxygens of Asp355, the pro-S oxygen of the scissile phosphate of the substrate, and a water molecule (Figure 2b). Less ideal liganding interactions are shown by the other carboxylate oxygen of Asp355 and carboxylate oxygens from Asp501 and Glu357. The Eu^{3+} ion is somewhat disordered (or poorly occupied), refining to a B factor of about 60 $Å^2$. No cation is observed at metal-ion site B. We have demonstrated that even a small, divalent cation could not bind to the active site in the presence of Eu^{3+} by performing a two-step soaking experiment. KF crystals were first soaked with Eu^{3+} and

substrate, exactly as before (see below). Crystals so treated were then transferred to a solution containing Eu^{3+}, substrate and 20 mM Mg^{2+} and allowed to soak for one hour. Previous crystallographic experiments [5,29] had established that this is sufficient time for divalent metal ions to bind to crystalline KF. After this soak, the crystals were cryostabilized and flash cooled, and diffraction data were subsequently collected. Difference electron-density maps derived from these data show no binding of Mg^{2+} at metal-ion site B and no differences in the binding of Eu^{3+} (data not shown).

We have concluded that Eu^{3+} and substrate ssDNA are bound at the KF exo active site concomitantly using three lines of evidence. First, both substrate and cation are clearly visible in electron-density maps even after the relatively short soaking time (1 h) used (Figure 2a). Second, the pro-S oxygen of the substrate's scissile phosphate ideally ligates the Eu^{3+} (distance = 2.3 Å). Finally, although ssDNA can bind to crystalline KF with no metal ions present using long soaks (1 week) or cocrystallization [3], no DNA can be observed at the KF exo active site in the absence of metal ions under our current (see below) quick-soaking conditions (C.A.B. and T.A.S., unpublished observations). The latter two facts illustrate that the cation is directly influencing the binding of substrate and, therefore, both must be concurrently present in the active site.

Figure 3

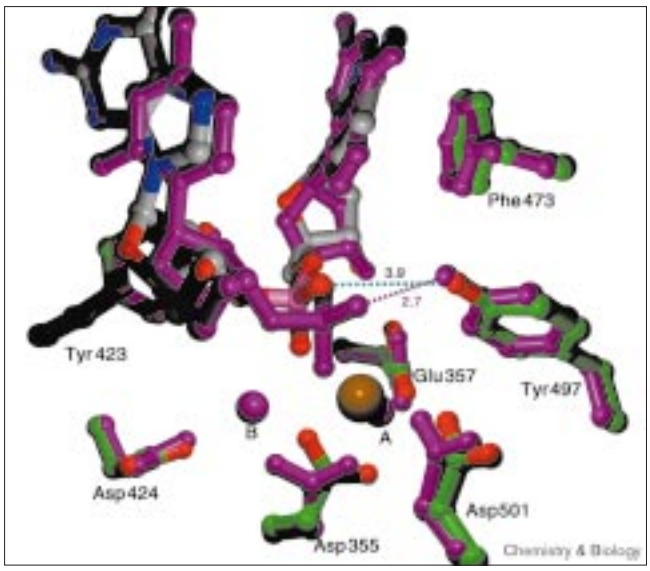

Superposition of the native and Eu^{3+}–substrate structures. The native complex is shown in purple and the Eu^{3+}–substrate structure is colored as in Figure 2b. The superposition was carried out by superimposing the Cα atoms of both structures in the exonuclease domain only using the program O [38]. The rmsd between the superimposed Cα atoms is 0.256 Å. This figure was made in VMD [41] and rendered using POV-Ray.

These arguments effectively rule out the mutually exclusive binding of substrate and metal ion to this active site that has been observed with Zn^{2+} and the S_p diastereomer of phosphorothioate DNA [5].

The arrangement of the substrate and metal ion in the Eu^{3+}–substrate complex differs substantially from that observed in a KF structure containing substrate and divalent cations [5]. Because this latter structure very nearly approximates the Michaelis complex for KF exo, we shall refer to it as the 'native complex'. Superposition of the exo domains of the two structures, which have been refined at similar resolutions, indicates that the positions of the scissile phosphates of the substrates differ by ~1.0 Å (Figure 3). As a consequence, a hydrogen bond observed in the native complex between the γ-OH of Tyr497 and the pro-R oxygen of the scissile phosphate is not formed in the Eu^{3+}–substrate complex. Overall, the electron density is poor for the substrate in the Eu^{3+}–substrate complex compared with that of the substrate of the native complex. The average B factor of atoms in the terminal dinucleotide in the Eu^{3+}–substrate complex is 53.1 $Å^2$, whereas it is only 32.9 $Å^2$ in the native complex. This might indicate either more disorder or lower occupancy of the DNA in the Eu^{3+}–substrate complex. The Eu^{3+} does not bind at exactly metal-ion site A. In the superposition, it is located 0.6 Å from the position of metal ion A in the native complex. Another major difference between the two structures is that metal ion B is absent in the Eu^{3+}–substrate complex, whereas it is clearly present in the native complex [5]. The binding of Eu^{3+} to the enzyme–substrate complex causes no large conformational change in the protein; indeed, most sidechains are in nearly identical positions in both complexes (Figure 3).

Other modes of Eu^{3+} binding

Other crystallographic analyses of Eu^{3+} bound to KF exo also reveal only a single cation bound at the active site. A difference electron-density map calculated at 3.8 Å resolution using diffraction data from KF crystals that were soaked in a solution containing 3 mM $Eu_2(SO_4)_3$•8 H_2O shows a single peak (8.5 σ) at the exonuclease active site near the native position of metal ion A (Figure 4a). Because of the modest resolution of this experiment, no water molecules could be seen ligating Eu^{3+}. Again, the identity of the difference electron-density peak was confirmed using the calculation of an anomalous difference electron-density map (Figure 4b), which shows a single 6 σ peak that coincides with the difference Fourier peak (compare Figure 4a with Figure 4b). No other Eu^{3+} peaks are evident in these analyses. When KF crystals are soaked in a solution containing Eu^{3+} and dTMP, a product of the exonuclease reaction, the cation binds to a different site. An anomalous difference electron-density map calculated at 3.5 Å resolution (Figure 5) shows that the single binding site for Eu^{3+} has shifted by approximately 3 Å

from those in Figures 2c,4b. The peak in Figure 5 is close to the native position of metal ion B. Again, the resolution of this analysis is not sufficient to locate water ligands to the Eu^{3+}. The density for the dTMP in this map is weak, even though it was included in the crystal soaking solution at a high concentration (14 mM).

Discussion

The results presented in this study provide a structural rationale for the observed inhibition [23] of KF exo by Ln^{3+}. Comparison of the Eu^{3+}–substrate and native complexes (Figure 3) shows that the position of the scissile phosphate of the DNA in the Eu^{3+}–substrate complex differs from its position in the native complex [5] by approximately one angström (Figure 3). The lone Eu^{3+} that binds near to metal-ion site A in this complex causes this movement by virtue of its larger ionic radius (approximately 0.4 Å larger than Mg^{2+} or Zn^{2+}) and its non-native binding site (approximately 0.6 Å away from metal-ion site A). In a previous study on KF exo [5], it has been established that a comparatively modest misplacement (0.6 Å) of the scissile phosphate from its native position inhibited the initial velocity of the enzyme 15–100-fold. It is probable, therefore, that the 1.0 Å shift observed in the Eu^{3+}–substrate complex is very deleterious to enzyme activity. Another inhibitory feature of the Eu^{3+}–substrate structure is the prohibition of metal-ion B binding (Figures 2,3). The absence of metal ion B from the KF exo active site eliminates enzyme activity [1,2,29] and so exclusion of this essential cation is undoubtedly a cause of the inhibition of KF exo by Eu^{3+}. The inhibition of KF exo by Eu^{3+} is, therefore, consistent with the two-metal-ion phosphoryl-transfer mechanism [3,4], which ascribes essential roles to both metal ions (Figure 1). In sum, Eu^{3+} inhibits KF exo by causing the misplacement of the substrate and by disallowing the binding of an essential catalytic cation.

Our results also provide clues to the mechanism by which Ln^{3+} ions inhibit other two-metal-ion phosphoryl-transfer enzymes. The 3′–5′ exonuclease domain of T4 DNA polymerase (T4 exo) is also inhibited by Eu^{3+} [23]. Because there is a high degree of structural and functional similarity between the active sites of KF exo and T4 exo [30], the same mechanism of inhibition is probably applicable to both. The polymerase activities of both KF and T4 DNA polymerase are destroyed by the presence of Eu^{3+} [23]. Because DNA polymerases appear to utilize a two-metal-ion mechanism that is analogous to the 3′–5′ exonucleases [7–10], the principles outlined above for KF exo and T4 exo inhibition probably hold for the polymerases as well.

The Eu^{3+}–substrate structure demonstrates that a lone cation can pre-empt a two-metal-ion binding site on an enzyme. This is probably caused by two factors in the KF exo system. First, the high positive charge on the Eu^{3+} might deter other cations from binding nearby (metal-ion site A is only 4 Å from metal-ion site B) [23]. Second, the ligation environment around metal ion site B is severely distorted. Asp355, which normally contributes ligands to both metal ions A and B, is interacting exclusively with Eu^{3+} (Figures 2b,3). This is presumably because of the high ligation number and charge of Eu^{3+}. In addition, the 1.0 Å misplacement of the scissile phosphate, a vital component of the ligation cage around metal ion B [1,4,5,29], further perturbs this metal-ion site. The binding of lanthanide (III) ions to two other two-metal-ion binding sites, those of thermolysin [31] and inositol monophosphatase [15,32], has been investigated using crystallography. In both cases, only a single Ln^{3+} binds to these sites. The causes of these phenomena are probably similar to those discussed above for KF exo.

Figure 4

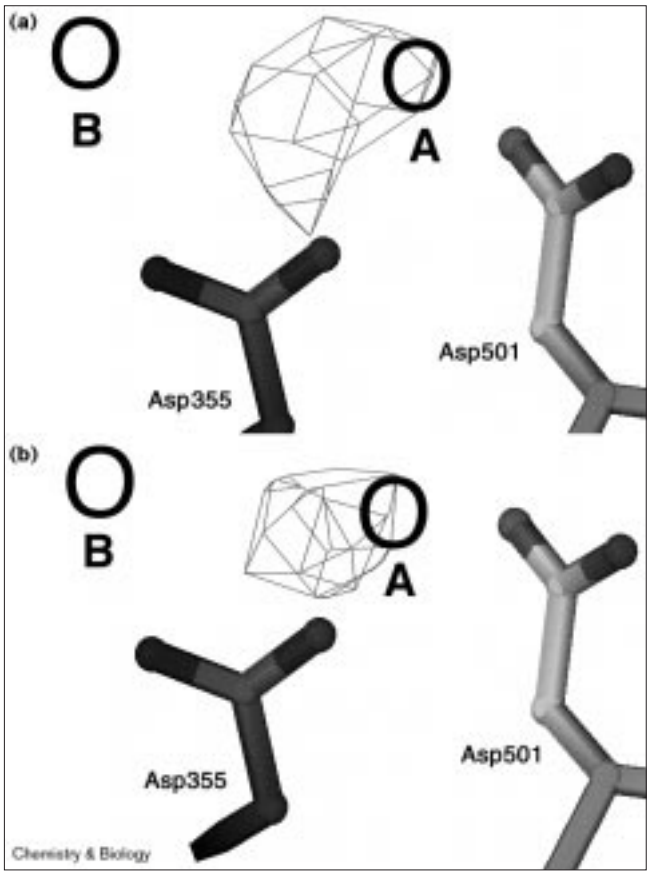

Eu^{3+} alone binding to KF exo. Both electron-density maps are superimposed on the rigid-body-refined coordinates obtained for KF. The black circles represent the normal positions of metal ions A and B. (a) Electron density for the Eu^{3+} ion. This F_o–F_c difference electron-density map, calculated using data from 7.0–3.8 Å, shows the location of a single Eu^{3+} binding at the KF exo active site. This is an 8.5 σ peak, and the map is contoured at 5 σ. (b) Anomalous difference density for Eu^{3+}. The anomalous difference density map was calculated using data from 10–3.8 Å. The contour level of the map is 4 σ.

It is probable that other large metal ions with a high ligation number will affect the structure and biochemistry of KF exo as Eu^{3+} does. X-ray crystallographic experiments (C.A.B. and T.A.S., unpublished observations) have demonstrated that a lone Tb^{3+} binds to this enzyme at the same site that Eu^{3+} does, and that it has the same effects on substrate and metal-ion B binding. This suggests that lanthanide (III) ions in general bind to KF exo and inhibit the enzyme comparably. Also, because Ln^{3+} ions are often used as probes for Ca^{2+} binding sites [25–28], the present study might offer insight into binding and inhibitory behavior [19] of Ca^{2+} with respect to KF exo. Unfortunately, we were unable to explore this notion in the KF exo system because the high sulphate concentration present in the crystal stabilization medium (2.8 M) is not compatible with the presence of greater than micromolar concentrations of free Ca^{2+} (for $CaSO_4$, $K_{sp} = 7.10 \times 10^{-5}$ [33]).

The rearrangements to the active site seen in the Eu^{3+}–substrate complex are in stark contrast to those observed in a structure of KF exo complexed to the S_p diastereomer of phosphorothioate DNA [5]. In this latter structure, which was solved in the presence of divalent metal ions, the pro-S oxygen of the substrate is replaced by a larger sulfur atom. The result is that metal ions are excluded from the active site, and the scissile phosphate is shifted slightly away from its native position. With Eu^{3+} present in the KF exo active site, both the large cation and the normal substrate are allowed to bind, albeit in non-native locations. What can account for these disparate reactions to larger atoms in the active site? A potential solution to this apparent paradox is found in the tripositive charge on the Eu^{3+} and the hydrogen bond between the γ-OH of Tyr497 and the pro-R oxygen of the scissile phosphate. In the case of the S_p diastereomer complex, accommodation of the larger sulfur atom and metal ion A would require the scissile phosphate to move away from Tyr497, weakening or breaking the hydrogen bond. This would destabilize the binding of the phosphorothioate substrate, perhaps causing it to dissociate. Instead, the hydrogen bond is kept and divalent cations do not occupy metal-ion site A. It is possible that the absence of the hydrogen bond does not have this effect in the Eu^{3+}–substrate complex because the loss of this interaction is compensated for by the larger Coulombic attraction between the scissile phosphate and the tripositive cation. It appears, therefore, that the mode of substrate binding observed in the Eu^{3+}–substrate complex is not solely caused by the position and size of Eu^{3+}; its tripositive charge also plays a role. The charge on Eu^{3+} influences, therefore, both the exclusion of metal ion B and the binding of substrate.

The results presented in this study provide structural insight into the previously published lanthanide (III) luminescence studies [23], which indicate that a lone Eu^{3+} binds to the active site of KF exo. The X-ray crystallographic studies that we have undertaken also indicate that a single Eu^{3+} binds here (Figures 2–5). In the KF–Eu^{3+} complex (Figure 4), which has been spectroscopically investigated [23], the cation binds in a position close to the previously characterized metal-ion site A [3–5]. The spectroscopic studies on this complex reveal two isomeric forms of Eu^{3+} binding to the KF exo active site, leading to the speculation that this is caused by two carboxylates or a water and a carboxylate competing for inner-sphere ligation to the Eu^{3+} [23]. Although the modest resolution (3.8 Å) of our KF–Eu^{3+} complex electron-density map does not allow us to define the ligation cage of the cation, we can comment on one aspect of the isomerism. It has been found that mutation of Asp424 to alanine eliminates one of the isomers [23]. Our results show clearly that Asp424 is not close enough to Eu^{3+} to be acting as an inner-sphere ligand. Given this fact and the structure of the KF exo active site, it is probable that the carboxylate moiety of Asp424 is hydrogen bonding to a water molecule that is in competition with a different carboxylate ligand. The loss of the carboxylate of Asp424 through mutation eliminates the hydrogen bonding partner of this water, thereby reducing the ability of this competing ligand to bind to the active site. This would explain the loss of one of the isomers in the mutant enzyme. The complex of KF, Eu^{3+} and dTMP was also studied spectroscopically [23]. Unfortunately, the addition of dTMP complicated the spectrum beyond interpretation. Our experiments using crystallography show that a single Eu^{3+} binds near to metal-ion site B in the presence of dTMP (Figure 5). The reason for the change in metal-binding behavior is not evident. It might be a consequence of the differences in amount and distribution of charge between dTMP (which has two negative charges on the

Figure 5

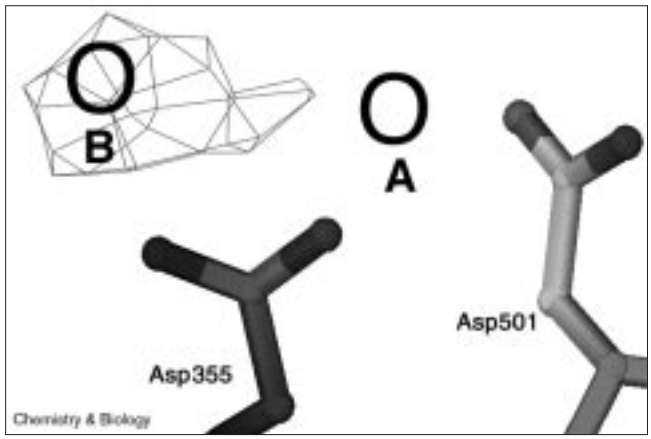

Eu^{3+} anomalous difference density in the presence of dTMP. The 6.5 σ Eu^{3+} peak is shifted from its previous location in Figures 4a,b. The map, contoured at 5 σ, was calculated using data from 10–3.5 Å and is superimposed on the rigid-body-refined coordinates obtained for the KF–Eu^{3+}–dTMP complex. Again, the circles show the normal positions for metal ions A and B.

phosphate) and substrate (one negative charge on the scissile phosphate). Although the spectroscopic studies point to the possibility of a second, weaker lanthanide-binding site on KF [23], our data do not reveal such a site. This could be because of the high-salt conditions of the crystal interfering with metal-ion binding, or due to the possibility that the high concentrations of lanthanides needed to observe such a site caused the enzyme to precipitate in the spectroscopic experiments, thus yielding a false binding signal [23]. On the basis of our results and the lanthanide (III) luminescence studies, it is evident that lanthanide (III) ions can be useful probes for identifying two-metal-ion binding sites on phosphoryl-transfer enzymes. As suggested by earlier researchers [23], however, the large ionic radius and tripositive charge of these cations can cause them to bind to such sites in a non-native manner.

Significance

This study using X-ray crystallography on the 3′–5′ exonuclease of Klenow fragment (KF) has provided the structural basis for understanding the mechanism by which lanthanides inhibit this enzyme. Comparison of the structure of the complex of KF exo, substrate ssDNA and Eu^{3+} to that of a previously determined native complex reveals that the lanathanide (III) ion (Ln^{3+}) slows the enzyme activity of KF exo in two ways: Eu^{3+} causes the position of the scissile phosphate to be incompatible with catalysis and Eu^{3+} causes the essential metal ion B to be barred from the active site. The latter is consistent with the two-metal-ion mechanism of phosphoryl transfer. These results also establish how a single Eu^{3+} bound at the KF exo active site abolishes the binding of metal ion B: the binding of Eu^{3+} causes numerous distortions to the KF exo active site that conspire to prevent metal ion B from binding. The principles of the binding and inhibitory behavior of Ln^{3+} elucidated for KF exo will probably extend to other two-metal-ion phosphoryl-transfer enzymes, for example DNA polymerases. Finally, when viewed in the light of previous spectroscopic investigations, our results demonstrate that Ln^{3+} ions might be used to detect metal-ion binding to two-metal-ion sites on phosphoryl-transfer enzymes, but that the nature of Ln^{3+} binding should not be interpreted as the native metal-ion binding state.

Materials and methods

Materials

KF was provided by Catherine Joyce. $Eu_2(SO_4)_3$•8 H_2O was obtained from Alfa Products. $Tb_2(SO_4)_3$·8 H_2O was obtained from Aldrich Chemical Company. All other chemicals, salts, and buffers were purchased from Sigma Chemical Corporation. Oligodeoxynucleotides were purchased from the Keck Biotechnology Center at Yale.

Methods

Crystal growth, storage, soaking and cryostabilization. Crystals were obtained using previously established conditions [34]. They were stored in a solution of 50 mM PIPES pH 7.0 and 2.8 M ammonium sulfate. For the Eu^{3+}-alone soak, crystals were transferred to a solution of 50 mM Tris pH 7.5, 2.8 M ammonium sulfate and 3.5 mM $Eu_2(SO_4)_3$•8 H_2O for 38 h. In addition to the above ingredients, the dTMP soak contained 14 mM dTMP. This soak was carried out for 24 h. Finally, the Eu^{3+}–substrate soaking solution contained 50 mM Tris pH 7.5, 2.8 M ammonium sulfate, 3.5 mM $Eu_2(SO_4)_3$•8 H_2O, and 1 mM 8-mer single-stranded oligodeoxynucleotide (sequence 5′-GCT-TACGC-3′, purified as described in reference [5]). Crystals were allowed to soak in this solution for 1 h. All crystals were subsequently placed into a cryostabilization solution that consisted of 16% (w/v) sucrose, 8% (w/v) xylitol, 4% (v/v) glycerol, 2.8 M ammonium sulfate, 50 mM PIPES pH 7.0, and 3 mM $Eu_2(SO_4)_3$·8 H_2O. After 5 min in this solution, crystals were supported on a loop of nylon and plunged into liquid propane. The liquid propane was frozen in liquid nitrogen and crystals were stored in this manner until data collection.

Data collection, processing and refinement. Intensity data were collected using an R-AXIS IV detector (Rigaku, Inc.) and a DIP-2000 detector (Molecular Structure, Inc.) at home X-ray sources, and an Area Detector Systems Corporation charge-coupled device detector at beamline A1 at Cornell High Energy Synchrotron Source (CHESS). Intensities were processed using the program DENZO [35] and scaled and merged with SCALEPACK [35]. Crystals belong to the space group $P4_3$, with approximate unit cell dimensions of a = b = 102 Å, c = 86 Å, $\alpha = \beta = \gamma = 90°$. A previously refined model of KF (J. Jäger and T.A.S., unpublished observations) was rigid-body refined into the new data using X-PLOR [36], because there was significant nonisomorphism between that model and the new data. After this, σ_A-weighted [37] $2F_o–F_c$ and $F_o–F_c$ electron-density maps were calculated to locate Eu^{3+} and product or substrate, if present. Electron-density maps and molecular models were visualized using O [38]. The only structure to be refined beyond this point was the Eu^{3+}–substrate complex. The low-resolution data were bulk-solvent corrected, and the model was subjected to iterative rounds of water placement, positional refinement, and individual B factor refinement in X-PLOR. The anomalous difference data for the Eu^{3+} alone and Eu^{3+}–substrate complexes were not collected in the standard inverse-beam fashion. Instead, the inherent redundancy in the data was used, and Fourier mates were separated using SCALEPACK. All anomalous difference density maps were calculated using the CCP4 suite of programs [39].

Accession numbers

The structure factors and coordinates of the Eu^{3+}–substrate complex have been deposited in the PDB with accession number 1QSL.

Acknowledgements

The authors wish to thank Paul Sigler, Nigel Grindley, and Fritz Eckstein for critical evaluations of the manuscript (in dissertation form), Catherine Joyce for helpful discussions and providing wild-type Klenow fragment, Xiaojun Chen Sun for purification of the enzyme, and Steven Bellon, Daniel Kaplan, and Yousif Shamoo for assistance with data collection. Some of the research in this paper was conducted at the CHESS, which is supported by the National Science Foundation under award DMR-9311772, using the Macromolecular Diffraction at CHESS (MacCHESS) facility, which is supported by award RR-01646 from the National Institutes of Health. We thank the personnel at CHESS beamlines A1 and F1 for their technical assistance. These studies were supported by NIH grant #GM39546 to T.A.S.

References

1. Derbyshire, V., *et al.*, & Steitz, T.A. (1988). Genetic and crystallographic studies of the 3′, 5′-exonucleolytic site of DNA polymerase I. *Science* 240, 199-201.
2. Derbyshire, V., Grindley, N.D.F. & Joyce, C.M. (1991). The 3′-5′ exonuclease of DNA polymerase I of *Escherichia coli*: contribution of each amino acid at the active site to the reaction. *EMBO J.* 10, 17-24.
3. Freemont, P.S., Friedman, J.M., Beese, L.S., Sanderson, M.R. & Steitz, T.A. (1988). Cocrystal structure of an editing complex of Klenow fragment with DNA. *Proc. Natl Acad. Sci. USA* 85, 8924-8928.
4. Beese, L.S. & Steitz, T.A. (1991). Structural basis for the 3′-5′ exonuclease activity of *Escherichia coli* DNA polymerase I: a two metal ion mechanism. *EMBO J.* 10, 25-33.

5. Brautigam, C.A. & Steitz, T.A. (1998). Structural principles for the inhibition of the 3′-5′ exonuclease activity of *Escherichia coli* DNA polymerase I by phosphorothioates. *J. Mol. Biol.* 277, 363-377.
6. Wilcox, D.E. (1996). Binuclear metallohydrolases. *Chem. Rev.* 96, 2435-2458.
7. Steitz, T.A. (1993). DNA- and RNA-dependent DNA polymerases. *Curr. Opin. Struct. Biol.* 3, 31-38.
8. Pelletier, H., Sawaya, M.R., Kumar, A., Wilson, S.H. & Kraut, J. (1994). Structures of ternary complexes of rat DNA polymerase β, a DNA template-primer, and ddCTP. *Science* 264, 1891-1903.
9. Doubli, S. & Ellenberger, T. (1998). The mechanism of action of T7 DNA polymerase. *Curr. Opin. Struct. Biol.* 8, 704-712.
10. Brautigam, C.A. & Steitz, T.A. (1998). Structural and functional insights provided by crystal structures of DNA polymerases and their substrate complexes. *Curr. Opin. Struct. Biol.* 8, 54-63.
11. Tesmer, J.J.G. & Sprang, S.R. (1998). The structure, catalytic mechanism and regulation of adenylyl cyclase. *Curr. Opin. Struct. Biol.* 8, 713-719.
12. Tesmer, J.J.G., Sunahara, R.K., Johnson, R.A., Gosselin, G., Gilman, A.G. & Sprang, S.R. (1999). Two-metal-ion catalysis in adenylyl cyclase. *Science* 285, 756-760.
13. Kim, E.E. & Wyckoff, H.W. (1991). Reaction mechanism of alkaline phosphatase based on crystal structures. *J. Mol. Biol.* 218, 449-464.
14. Davies, J.F., Hostomska, Z., Hostomsky, Z., Jordan, S.R. & Matthews, D.A. (1991). Crystal structure of the ribonuclease H domain of HIV-1 reverse transcriptase. *Science* 252, 88-95.
15. Bone, R., Frank, L., Springer, J.P. & Atack, J.R. (1994). Structural studies of metal binding by inositol monophosphatase: evidence for two-metal ion catalysis. *Biochemistry* 33, 9468-9476.
16. Pollack, S.J., *et al.*, & Broughton, H.B. (1994). Mechanism of inositol monophosphatase, the putative target of lithium therapy. *Proc. Natl Acad. Sci. USA* 91, 5766-5770.
17. Atack, J.R., Broughton, H.B. & Pollack, S.J. (1995). Structure and mechanism of inositol monophosphatase. *FEBS Lett.* 361, 1-7.
18. Steitz, T.A. & Steitz, J.A. (1993). A general two-metal-ion mechanism for catalytic RNA. *Proc. Natl Acad. Sci. USA* 90, 6498-6502.
19. Lehman, I.R. & Richardson, C.C. (1964). The deoxyribonucleases of *Escherichia coli*: IV. An exonuclease activity present in purified preparations of deoxyribonucleic acid polymerase. *J. Biol. Chem.* 239, 233-241.
20. Mullen, G.P., Serpersu, E.H., Ferrin, L.J., Loeb, L.A. & Mildvan, A.S. (1990). Metal binding to DNA polymerase I, its large fragment, and two 3′, 5′-exonuclease mutants of the large fragment. *J. Biol. Chem.* 265, 14327-14334.
21. Han, H., Rifkind, J.M. & Mildvan, A.S. (1991). Role of divalent cations in the 3′, 5′-exonuclease reaction of DNA polymerase I. *Biochemistry* 30, 11104-11108.
22. Derbyshire, S.V. (1990). Studies on the 3′–5′ exonuclease of DNA polymerase I of *Escherichia coli*. Ph.D. Thesis, Yale University, New Haven, CT.
23. Frey, M.W., Frey, S.T., de W. Horrocks, W, Jr., Kaboord, B.F. & Benkovic, S.J. (1996). Elucidation of the metal-binding properties of the Klenow fragment of *Escherichia coli* and bacteriophage T4 DNA polymerase by lanthanide (III) luminescence spectroscopy. *Chem. Biol.* 3, 393-403.
24. Komiyama, M., Matsumura, K. & Matsumoto, Y. (1992). Unprecedentedly fast hydrolysis of the RNA dinucleoside monophosphates ApA and UpU by rare earth metal ions. *J. Chem. Soc., Chem. Commun.* 640-641.
25. de W. Horrocks, W., Jr. & Sudnick, D.R. (1979). Lanthanide ion probes of structure in biology. Laser-induced luminescence decay constants provide a direct measure of the number of metal-coordinated water molecules. *J. Am. Chem. Soc.* 101, 334-340.
26. Darnall, D.W. & Birnbaum, E.R. (1970). Rare earth metal ions as probes of calcium ion binding sites in proteins. Neodymium (III) acceleration of the activation of trypsinogen. *J. Biol. Chem.* 245, 6484-6486.
27. Smolka, G.E., Birnbaum, E.R. & Darnall, D.W. (1971). Rare earth metal ions as substitutes for the calcium ion in *Bacillus subtilis* amylase. *Biochemistry* 10, 4556-4561.
28. Darnall, D.W. & Birnbaum E.R. (1973). Lanthanide ions activate α-amylase. *Biochemistry* 12, 3489-3491.
29. Brautigam, C.A., Sun, S., Piccirilli, J.A. & Steitz, T.A. (1999). Structures of normal single-stranded DNA and deoxyribo-3′-*S*-phosphorothiolates bound to the 3′–5′ exonucleolytic active site of DNA polymerase I from *Escherichia coli*. *Biochemistry* 38, 696-704.
30. Wang, J., Yu, P., Lin, T.C., Konigsberg, W.H. & Steitz, T.A. (1996). Crystal structures of an NH_2-terminal fragment of T4 DNA polymerase and its complexes with single-stranded DNA and with divalent metal ions. *Biochemistry* 35, 8110-8119.
31. Matthews, B.W. & Weaver, L.H. (1974). Binding of lanthanide ions to thermolysin. *Biochemistry* 13, 1719-1725.
32. Bone, R., Springer, J.P. & Atack, J.R. (1992). Structrure of inositol monophosphatase, the putative target of lithium therapy. *Proc. Natl Acad. Sci. USA* 89, 10031-10035.
33. Lide, D.R. (1990). CRC Handbook of Chemistry and Physics, (71st edn), CRC Press, Boca Raton.
34. Brick, P., Ollis, D. & Steitz, T.A. (1983). Crystallization and 7 Å resolution electron density map of the large fragment of *Escherichia coli* DNA polymerase I. *J. Mol. Biol.* 166, 453-456.
35. Otwinowski, Z. & Minor, W. (1997). Processing of X-ray diffraction data collected in oscillation mode. *Methods Enzymol.* 276, 307-325.
36. Brünger, A.T. (1992). *X-PLOR, Version 3.1*. Yale University Press, New Haven, CT.
37. Read, R.J. (1986). Improved Fourier coefficients for maps using phases from partial structures with errors. *Acta Crystallogr. A* 42, 140-149.
38. Jones, T.A., Zou, J.-Y., Cowan, S.W. & Kjeldgaard, M. (1991). O. *Acta Crystollogr. A* 47, 110-119.
39. Collaborative Computational Project, Number 4 (1994). The CCP4 suite: programs for protein crystallography. *Acta Crystallogr. D* 50, 760-763.
40. Hodel, A., Kim, S.-H. & Brünger, A.T. (1992). Model bias in macromolecular crystal structures. *Acta Crystollogr. A* 48, 851-859.
41. Humphrey, W., Dalke, A. & Schulten, K. (1996). VMD-visual molecular dynamics. *J. Mol. Graphics* 14, 33-38.

Because *Chemistry & Biology* operates a 'Continuous Publication System' for Research Papers, this paper has been published via the internet before being printed. The paper can be accessed from http://biomednet.com/cbiology/cmb – for further information, see the explanation on the contents pages.